Fuel 258 (2019) 116195

Contents lists available at ScienceDirect

Fuel

journal homepage: www.elsevier.com/locate/fuel

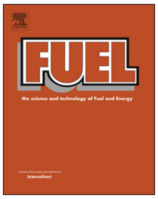

Full Length Article

Ketone solvent as a wettability modifier for improved oil recovery from oil-wet porous media

Mingyuan Wang, Gayan A. Abeykoon, Francisco J. Argüelles-Vivas, Ryosuke Okuno*

Hildebrand Department of Petroleum and Geosystems Engineering, The University of Texas at Austin, 200 E. Dean Keeton Street, Stop C0300, Austin, TX 78712, USA

ARTICLE INFO

Keywords:
Ketone solvent
Wettability alteration
3-Pentanone
Imbibition
Improved oil recovery
Interfacial tension

ABSTRACT

The main objective of this research is to investigate a novel class of oxygenated solvents that can enhance the oil recovery from oil-wet rocks by multiple mechanisms, such as wettability alteration, oil-viscosity reduction, and oil swelling, in the presence of brine (connate water and/or fracturing water). The compound studied for the first time in this research is 3-pentanone (3p), a symmetric short ketone that can partition into both oil and brine at reservoir conditions. It can act as a solvent by itself, but this paper is focused on the potential mechanisms of oil recovery when an aqueous solution of 1.1 wt% 3p in reservoir brine (3pRB) is in contact with oil and oil-wet rock.

Results show that the average contact angle of oil droplets on oil-aged calcite surfaces was rapidly reduced to 26° with 3pRB, in contrast to 123° with RB, without affecting the oil/brine interfacial tension. Spontaneous imbibition results show that the oil recovery factor reached 50.0% with 3pRB and 10.0% with RB at Day 3. The final recovery factor was 51.0% with 3pRB and 12.0% with RB. The subsequent forced imbibition determined the Amott index to water of 0.76 with 3pRB and 0.23 with RB, indicating a clear, positive impact of 3pRB on oil recovery by water imbibition in the cores tested. The main mechanism of oil recovery by 3pRB in this research is the wettability change as demonstrated by the contact-angle experiment.

1. Introduction

Horizontal drilling and multi-stage hydraulic fracturing have made it possible to recover oil from tight formations at economically feasible production rates. However, tight oil reservoirs often show a rapid decline in production rate. For example, a decline of 60%–70% in oil production rate within a first year has been reported for tight formations in the Eagle Ford [1,2]. Primary recovery factors in tight oil reservoirs are typically lower than 10% [2–7].

In addition to their low permeabilities, the oil recovery from tight oil reservoirs is likely affected by heterogeneous petrophysical properties at different scales and phase distribution [8,9]. The diversity of minerals and high total organic content (TOC) have been studied for various shale plays [7,10,11]. For example, a rock sample from Wolfcamp contained 13 wt% quartz, 15 wt% clays, 46 wt% calcite, 19 wt% dolomite, 4 wt% feldspar, and 3 wt% pyrite with 5–6 wt% TOC in Alvarez et al.'s study [12].

Different minerals show different wettability states. Quartz tends to show a water-wet state because the surface is negatively charged [13,14]. In contrast, calcite tends to show an oil-wet state, because the positively charged surfaces can adsorb negatively charged oil components (naphthenic acids) [13,14]. In addition, the presence of organic matter also causes the rock to be in an oil-wet state. Alvarez and Schechter reported that most tight oil reservoirs are originally intermediate-wet to oil-wet, which affects the multicomponent transport phenomena in tight formations in a complicated manner [14].

Various methods have been studied for recovering oil from mixed- to oil-wet rocks and altering their wettability state to more water-wet, such as surfactant-solution injection, alcohol-solution injection, and low-salinity water (LSW) injection [11,12,15–17]. These wettability alteration agents are injected to facilitate water imbibition into tight rock matrices [11].

Surfactant-solution injection for improved oil recovery in tight oil reservoirs has been studied by many researchers [7,11,12,16,18–23]. The mechanisms of improved tight-oil recovery by the surfactant-solution injection include wettability alteration and interfacial tension (IFT) reduction between the oleic and aqueous phases [7,11,12,16,20,21,24]. Alvarez et al. indicated that the IFT reduction is important, but the IFT should not reach an ultralow value (e.g., 10^{-3} mN/m) for improved oil recovery in tight reservoirs [11,16]. Kathel et al. also stated that an ultra-low IFT limits the surfactant imbibition rate and, therefore, oil recovery [7,20]. Adibhatla et al.

---

* Corresponding author.
E-mail address: okuno@utexas.edu (R. Okuno).

https://doi.org/10.1016/j.fuel.2019.116195
Received 27 July 2019; Received in revised form 7 September 2019; Accepted 9 September 2019
Available online 17 September 2019
0016-2361/

Nomenclature

3p	3-pentanone
3pRB	3-pentanone solution in reservoir brine
d	core diameter
H	height of the core
k	permeability
L	length of the core
N_B	Bond number
t	time
u	injection rate
ϕ	porosity
σ	interfacial tension
ρ	density
3p	3-pentanone
3pRB	3-pentanone solution in reservoir brine
IFT	interfacial tension
^{1}H NMR	proton nuclear magnetic resonance
LSW	low-salinity water
PVI	pore volume(s) injected
RB	reservoir brine
TOC	total organic content
t_d	dimensionless time
μ_o	oleic phase viscosity
μ_w	aqueous phase viscosity

demonstrated that oil recovery rate decreases with decreasing IFT when the wettability is altered by a surfactant solution [25,26]. Tu and Sheng showed similar results through novel imbibition experiments at high pressure [27]. They indicated that oil recovery from a tight reservoir can be improved by inducing wettability alteration with a moderate IFT reduction. This seems to be a marked difference from the conventional surfactant-enhanced oil recovery, which depends on achieving ultra-low IFT during the convective oil displacement [28]. More exploratory studies should be done for surfactant-based methods for tight oil reservoirs. Several studies indicated that the diffusion of surfactants is an important controlling parameter in oil recovery from tight rocks because surfactants are typically large molecules [29]. However, some ultra-short hydrophobe surfactants are relatively short, and can be viewed as surface-active cosolvents. Their applications are being studied for enhanced oil recovery [30].

Different types of surfactants (e.g., anionic, non-ionic, and cationic surfactants) have been compared in terms of wettability alteration and improve oil recovery [11,12,16,21,31,32]. Alvarez et al. showed that both anionic and non-ionic surfactants changed the wettability of carbonate and siliceous shale samples, but the former performed better than the latter [21]. Liu et al. presented that non-ionic surfactants did not affect the wettability of siliceous shale, but anionic surfactants altered its wettability [31].

Recently, Lu et al. presented a study of 1-pentanol solution for wettability alteration [17]. Contact angle measurements showed that 1 wt% 1-pentanol solution can significantly decrease the contact angle of a petroleum fluid on calcite. The effect was pronounced with 0.5 wt% 1-pentanol at high NaCl or $MgCl_2$ concentrations. They explained that this wettability alteration came from the accumulation of 1-pentanol in the thin brine film between oil and the rock surface.

LSW injection has been widely studied for conventional reservoirs, but also recently for tight oil reservoirs [7,33]. Austad et al. proposed a mechanism of wettability alteration via synergistic interactions of Ca^{2+}, Mg^{2+}, and $SO_4{}^{2-}$ ions in seawater to remove the carboxylic acid groups of oil adsorbed in chalk cores [34]. The mechanism relies on the polar-polar interaction between negatively charged sulfate ions with positively charged rock surfaces that brings the wettability towards a more water-wet state.

Inspired by this mechanism through the action of sulfate ions, we started searching for practical solvents that can weaken the interaction of polar oil components with positively charged rock surfaces. Since the carbonyl oxygen of ketones is electron-rich with a partially negative charge, we hypothesized that ketone solvents might be able to alter the rock wettability towards a water-wet state. This hypothesis was successfully tested with acetone in our initial screening of ketone solvents. However, the oleic phase was found to become highly viscous in the presence of water and acetone, as is the case with alcohol/water/oil mixtures [35–37]. Then, the subsequent optimization reached a more favorable balance of the affinities for crude oil and brine with a larger alkyl side chain groups than acetone. On the basis of our exploratory study, this paper presents an investigation focused on 3-pentanone that was found to act as a wettability alteration agent and also as a miscible solvent with crude oil at reservoir conditions.

3-Pentanone (3p) is a symmetric ketone with the chemical formula of $C_5H_{10}O$ (Fig. 1). It is a colorless liquid at standard conditions, non-toxic, and widely used in the food industry. 3-Pentanone acts as a usual solvent in the oleic phase when the concentration is beyond the solubility limit in the aqueous phase. A significant portion of the 3p will partition from the aqueous phase to the oleic phase when a 3p aqueous solution is brought in contact with an oleic phase, regardless of the 3p concentration in the aqueous phase. Furthermore, it can interact with oil-wet surfaces, causing the wettability to a more water-wet state as will be presented later in this paper.

This paper is focused on the application of 3p as a sole additive to reservoir brine (RB) with no modification to RB's ionic composition and salinity. Use of a 3p solution in RB (3pRB) is compared with use of RB alone to see the effect of the presence of 3p in RB on oil recovery. The subsequent sections present the materials and methods used for this research, key results, and conclusions.

2. Materials and methods

This section presents the materials and methods used for the investigation of the potential oil recovery mechanisms by 3pRB, such as wettability alteration and oil viscosity reduction. This section also presents fundamental data, such as properties of the oil, RB, 3p, and 3pRB, and the aqueous stability of 3pRB.

2.1. Reservoir fluid properties

A crude oil sample was taken from a tight oil reservoir in Texas. The reservoir temperature is 347 K. The reservoir brine (RB) with a salinity of 68722 ppm was prepared in the lab by using available field data. Table 1 summarizes properties of the oil sample. Table 2 shows the ionic composition of RB. The density and viscosity of RB were measured to be 1030 kg/m^3 and 0.56 cp at the experimental conditions in this research (347 K and atmospheric pressure).

2.2. 3-Pentanone properties

A sample of 3p had a purity greater than 99% (Sigma-Aldrich).

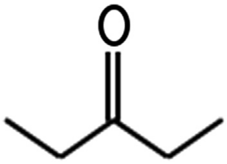

Fig. 1. Molecular structure of 3-pentanone.

Table 1
Properties of the crude oil sample used in this research.

Molecular weight, g/mol		186
Density, kg/m^3		822.5 (at 288.71 K)
SARA, wt%	Saturates	76.7
	Aromatics	20.1
	Resins	3.2
	Asphaltenes (pentane insoluble)	less than 0.1

Table 2
Composition of the reservoir brine (RB) used in this research (68722 ppm). The density of RB was measured to be 1030 kg/m^3 at 347 K and atmospheric pressure.

Cations	ppm	Anions	ppm
Na$^+$	25,170	Cl$^-$	41,756
K$^+$	210	SO$_4$$^{2-}$	108
Ca^{2+}	1292		
Mg^{2+}	187		

Vapor pressures of 3p measured by Collerson et al. [38] show that 3p is close to n-heptane in terms of volatility; that is, it is possible to inject 3p as part of the gaseous injection fluid. The density of 3p is 760 kg/m^3 at the experimental conditions in this research (347 K and atmospheric pressure), according to Daubert and Danner [39]. Fig. 2 shows single-phase mixtures of 3p with the crude oil at room temperature. No phase separation was observed for the overall concentrations of 3p tested (between 30 wt% and 95 wt%).

The aqueous stability was confirmed for 3p in RB (Table 2) at 347 K (Fig. 3). No salt precipitation was observed for the overall concentrations of 3p tested (0.1 wt%–40 wt%). A phase separation occurred with increasing concentration of 3p. There was a very small amount of excess 3p-rich phase at 2- wt% 3p. These results indicate that the 3p solubility limit in RB is lower than the aqueous stability limit at 347 K, which makes 3p suitable as an additive to a RB-based injection fluid. Quantitative ^{1}H NMR analysis indicated that the solubility limit of 3-pentanone in RB at 347 K is 1.1 wt%. This defined the maximum concentration of 3p in 3pRB tested in this research. In comparison, the 3p solubility in deionized water at 347 K was measured to be 2.59 wt% in this research. Solubilities of water in 3p were reported by Stephenson [40].

The densities of 1.1- wt% 3pRB and 0.8- wt% 3pRB were measured to be 1030 kg/m^3 at the experimental conditions in this research (347 K and atmospheric pressure). The viscosity of 1.1- wt% 3pRB was measured to be 0.52 cp by a rheometer at 347 K and atmospheric pressure. These values will be used in Section 2.4.

2.3. Contact-angle experiments

Contact-angle experiments were performed by using polished flat calcite surfaces. Calcite was used because it is one of the major minerals often observed in tight formation rocks. Its positively charged surfaces can be made oil wet by adsorption of negatively charged oil components. The polished calcite pieces of approximate dimensions $5 \times 2 \times 0.5$ cm^3 were washed with deionized water. Then, the air-dried calcite pieces were aged in RB (Table 2) for 1 day at 347 K and air dried. Next, the brine-aged calcite pieces were aged in crude oil (Table 1) for at least 5 weeks, and then in a heavy oil for at least 1 week at 347 K. The heavy oil was used to ensure that the calcite surfaces are oil-wet. After the aging, the calcite pieces were retrieved and any excess oil was carefully removed from the surfaces.

The contact-angle experiments were performed with two aqueous solutions, RB and 1.1- wt% 3pRB (the solubility limit) at 347 K. The solutions were degasified inside an oven at 368 K for at least 2 days. Then, two glass chambers were prepared, each of which contained one aqueous solution and one calcite piece. The glass chambers were placed in an oven at 368 K for 1 h to confirm that no gas bubble appeared. Then, two droplets of oil (Table 1) were placed on the bottom surface of each calcite piece in each glass chamber. After the placement of oil droplets, 3p was added to a glass chamber to make the 3p overall concentration of 8 wt%. The glass chambers were then tightly closed and placed in the oven at 347 K. Since 8 wt% was beyond the 3p solubility in RB at 347 K (1.1 wt%), an excess 3p phase was present above the 1.1- wt% 3p aqueous solution (Fig. 3). This excess 3p phase served as a reservoir that maintained the concentration of 3p in the aqueous phase at the 3p solubility limit as it dissolved into the oil during the experiment. This procedure avoided several issues that would occur if RB and the added 3p were mechanically mixed before the chamber was placed in the oven. For example, the air dissolution would occur if the mixture was mechanically stirred. Also, nucleation of the 3p phase might affect oil droplets on calcite surfaces upon a phase separation with increasing temperature.

Photos of oil droplets were taken at the initialization of the experiment and every several hours for up to three days. The contact angles of both sides of each oil droplet were measured using onscreen protractor software. An average contact angle and standard deviation were then calculated and plotted with respect to time for each aqueous solution tested.

2.4. IFT experiments

The IFT experiments were performed by use of a spinning drop tensiometer (SDT, Krüss, Germany) at 347 K. This device can measure IFTs between 10^{-6} and 2000 mN/m with a resolution of 10^{-6} mN/m. During the measurement, the denser phase was placed into a horizontal tube first, and then a droplet of the less dense phase was placed into the horizontal tube while the tube was rotating. The droplet was deformed owing to the rotation, which was visualized by using a high power monochromatic light-emitting diode and stroboscope. The shape of a droplet spinning in the capillary tube was recorded by a high-resolution camera. The ADVANCE™ software was then used to analyze the shape of a droplet and calculate an IFT value, using the densities of the two phases at 347 K.

IFT values were measured for four systems: (1) crude oil and RB, (2) 3p and 1.1- wt% 3pRB, (3) crude oil and 1.1- wt% 3pRB, and (4) crude oil diluted by 18.6 wt% 3p and 0.8- wt% 3pRB. System 1 was at phase equilibrium. A certain level of mass transfer was expected during the IFT measurement for the other three pseudo-binary systems. In system 2, water could transfer from 1.1- wt% 3pRB to the 3p-rich phase. An IFT was estimated by using the densities of 3p and 1.1- wt% 3pRB. In system 3, 3p could be transferred from RB to crude oil, which reduced the density of the oleic phase. Therefore, the upper-limit and lower-limit density values were assigned for the oleic phase to calculate a

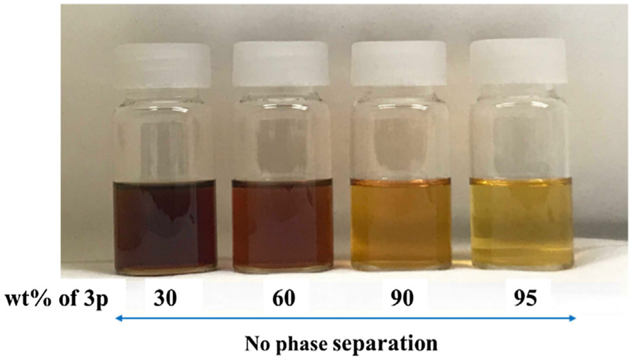

Fig. 2. Mixtures of 3p with the crude oil at room temperature. The overall concentrations of 3p tested are from 30 wt% to 95 wt%. No phase separation was observed.

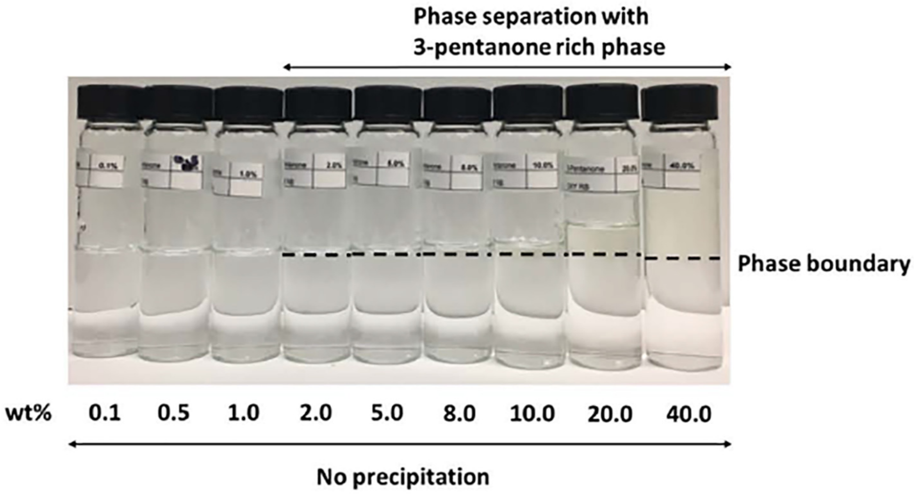

Fig. 3. Aqueous stability test of the reservoir brine (Table 2) with 3-pentanone at 347 K. The overall concentrations of 3-pentanone tested are from 0.1 wt% to 40 wt %. No salt precipitation was observed because the solubility of 3-pentanone in RB is only 1.1 wt% at 347 K as measured by quantitative ^{1}H NMR analysis.

possible range of IFTs for this system. System 4 was tested to validate the range of IFT values estimated for system 3. To this end, an IFT was determined by using the density of the crude oil that was diluted by 18.6 wt% 3p and the density of 0.8- wt% 3pRB at 347 K. These concentrations correspond to the values from the samples taken from the oleic and aqueous phases that were present in the Amott cell after the imbibition experiment as will be explained in Section 3.4.

2.5. Density and viscosity experiments

Fig. 4 shows a schematic of the experimental set up for density and viscosity experiments. The system consists mainly of automated pumps, a sample accumulator, an in-line fluid densitometer, an in-line viscometer, an oven, and an effluent accumulator. The pump (Teledyne ISCO 100DX) maintained the system pressure automatically by water.

In the density measuring cell (Anton Paar DMA-HPM), fluid's density is measured in a U-shaped tube, in the range from 0 to 3000 kg/m^3. The instrument precision of the density meter is ± 1 kg/m^3. Anton Paar DMA-HPM uses the method of oscillating U-tube for its density measurement, in which the sample's density is calculated from the sample's period of oscillation [41]. The in-line viscometer (ViscoPro 2100) measures the viscosity of a fluid in the range from 0.2 to 2 cp. The instrument precision of the viscometer is ± 0.02 cp and repeatability is ± 0.5% of the reading. During the viscosity measurement, the magnetic piston is surrounded by the fluid sample and oscillates under magnetic force [42]. The sample's viscosity is calculated from the time required for the piston to complete a two-way cycle [42]. The viscometer and density meter were placed in a Despatch oven (model LAC2-18-8). Light-emitting diode screens that display measured data from the fluid densitometer and viscometer were connected outside the oven. The absolute pressure of the system was measured with a pressure gauge (Omega PX459-2.5KGI-EH).

Densities and viscosities were measured for the following mixtures of crude oil and 3p: 81.4 wt% crude oil and 18.6 wt% 3p (33 mol% 3p), 59.0 wt% crude oil and 41.0 wt% 3p (60 mol% 3p), and 35.1 wt% crude oil and 64.9 wt% 3p (80 mol% 3p). Each mixture was mixed in a glass bottle with a magnetic mixer before placing it in the accumulator.

Before each measurement, the system was cleaned thoroughly with

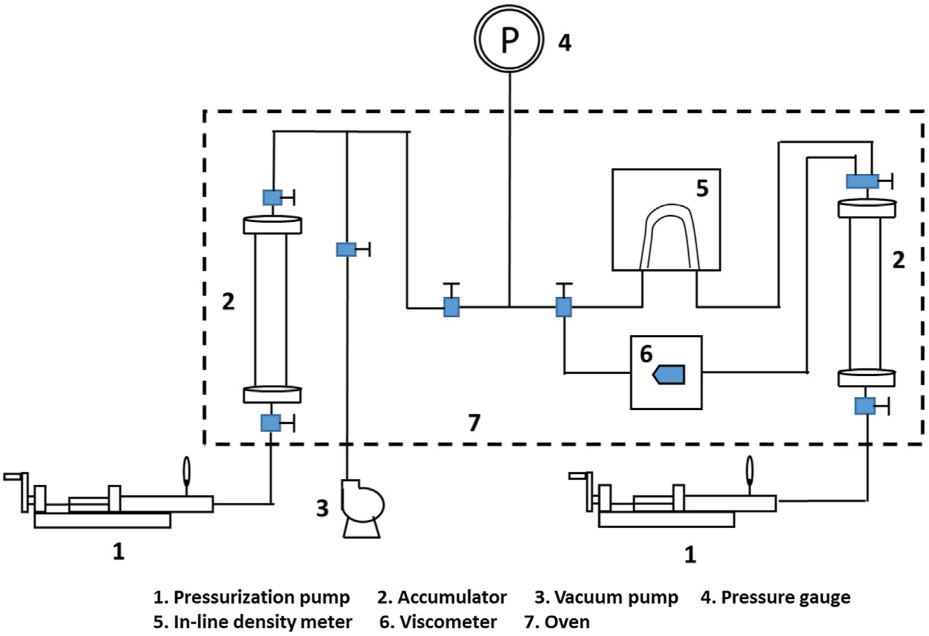

Fig. 4. Schematic of the experimental set up for the density and viscosity experiment (Section 2.5).

toluene. Then, the system was dried by air and evacuated. Next, the fluid mixture was pumped into the system from the accumulator. Then, the temperature in the oven was increased to 347 K. When the temperature in the oven was stable, the mixture was measured for viscosities and densities at different pressures, ranging from 101 kPa to 10342 kPa.

2.6. Spontaneous imbibition

Spontaneous imbibition experiments were performed using Amott cells at 347 K to quantify the effect of 3p on oil recovery through water imbibition. Indiana limestone cores with a length of 0.127 m and a diameter of 0.0254 m were used for this research. Limestone cores can represent an oil-wet condition by aging them in oil. The inverse Bond number (N_B^{-1}) with these cores ranged from 33 to 38:

$$N_B^{-1} = C\frac{\sigma\sqrt{\phi/k}}{\Delta\rho g H}. \tag{1}$$

An imbibition process is said to be capillary-force dominated when $1/N_B$ is larger than 5 [43]. That is, the imbibition in this research was capillary-force dominated so that the experiment could capture the effect of wettability on oil recovery [24,43]. In Eq. (1), N_B is Bond number, C is 0.4 for the capillary tube model, σ is interfacial tension, ϕ is porosity, k is permeability, $\Delta\rho$ is the density difference between the aqueous and oleic phases, and H is the height of the core [44].

The cores were saturated with RB and oil. Fig. 5 shows a schematic of the core-flooding system used. It consists of two accumulators for RB and crude oil, a pump, a Hassler type core-holder, a vacuum pump, a hydraulic manual pump to maintain the overburden pressure, a differential pressure gauge, and cylinders.

After a core was placed in the core holder, the system was evacuated. Then, the core was saturated with RB. The effective porosity of the core was determined by subtracting the system's dead volume (3.65 cm^3) from the volume injected. Then, the permeability of the core was determined by RB injection rates and differential pressures. Next, the crude oil (Table 1) was injected into the core at 50 cm^3/h. After the oil breakthrough, the injection rate was increased to 100 cm^3/h to minimize the capillary end effect. The injection of crude oil at 100 cm^3/h was continued until the water production became unmeasurable. A residual water saturation was estimated from the produced brine volume. Table 3 summarizes the measured porosity, permeability, water saturation and oil saturation for the core samples used in the imbibition experiment. Finally, the oil-saturated cores were placed in a container filled with the crude oil for at least three weeks at 347 K. Similar initial water/oil saturations were achieved with Indiana limestone cores in the literature [45,46].

Table 3
Properties of the two cores used for the imbibition experiments. RB and 3pRB stand for reservoir brine and 1.1- wt% 3-pentanone in RB, respectively.

	Core for the RB case	Core for the 3pRB case
Porosity	0.196	0.200
Permeability, mD	28.0	35.1
Water saturation	0.57	0.54
Oil saturation	0.43	0.46

The two cores prepared (Table 3) were used for imbibition experiments with the following aqueous solutions: RB and 1.1- wt% 3pRB. To this end, RB and a mixture of 8 wt% 3p and 92 wt% RB were prepared one day prior to the imbibition experiment and placed in an oven at 347 K to minimize the amount of dissolved gas. The mixture of 8 wt% 3p and 92 wt% RB showed an excess 3-p phase as the overall 3p concentration was beyond the solubility of 3p in RB at 347 K. In the preparation of the imbibition experiment, core samples were placed inside the imbibition cells first. Then, RB and the 3p/RB mixture were carefully poured into the respective Amott cells. This was done without cooling the solutions and inside a heated oven to minimize any oil recovery due to thermal expansion of fluids. Then, the excess 3p phase that was present above 1.1 wt% 3pRB (the 3p solubility in RB at 347 K) was carefully removed from the Amott cell prior to the imbibition experiment. Note that the removal of the excess 3p phase was not done for the contact angle measurement for 1.1- wt% 3pRB (Section 2.3), but was done here to avoid the mixing of the recovered oil with the excess 3p phase present in the glass-tube part of the Amott cell. That is, the 3p concentration in the aqueous phase was not kept at the solubility limit (1.1 wt%) in this imbibition experiment as 3p was gradually dissolved in the oleic phase. During the experiment, no attempt was made to detach oil drops from the core surfaces.

The recovered oleic-phase volume was periodically measured during the imbibition experiment at 347 K. For the 3pRB case, 3p could be transferred from the aqueous to the oleic phase; therefore, the amount of 3p in the recovered oil was measured by quantitative ^{1}H NMR analysis and subtracted from the amount of the oleic phase recovered in the Amott cell. The same NMR analysis was performed for the 3p aqueous solution inside the Amott cell after the experiment.

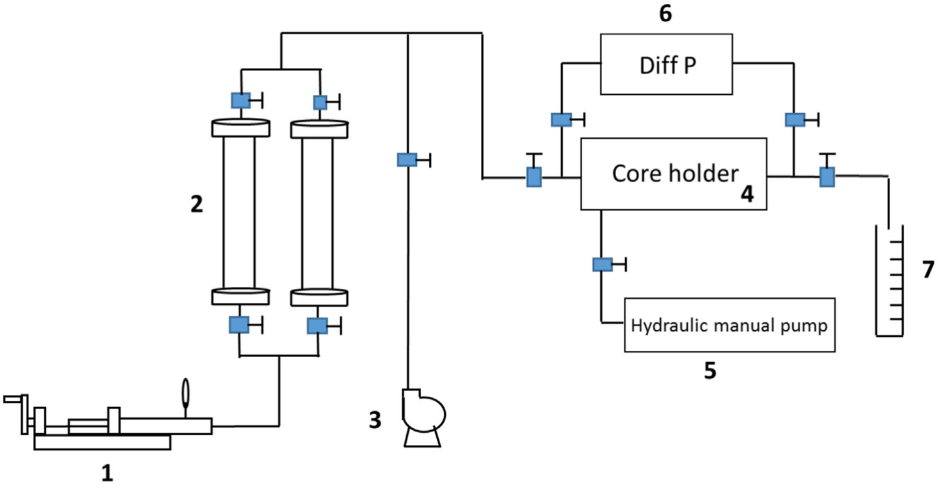

1. Pressurization pump 2. Accumulators 3. Vacuum pump 4. Hassler type core-holder
5. Hydraulic manual pump 6. Differential pressure gauge 7. Graduating cylinder

Fig. 5. Schematic of the experimental set up for saturating cores (Section 2.6).

2.7. Forced imbibition

The spontaneous imbibition (Section 2.6) was followed by forced imbibition for the same cores with their corresponding displacing fluids, RB and 1.1- wt% 3pRB, at 347 K. Fig. 6 shows a schematic of the experimental set up for this forced imbibition. It consists of an accumulator for the aqueous phase to be injected, a pump, a Hassler type core-holder, a hydraulic manual pump to maintain the overburden pressure, a differential pressure gauge, and an oven. The connecting lines were filled with the displacing fluid prior to the placement of a core inside the core holder.

Before the forced imbibition, the recovered oleic phase and the remaining aqueous solution in the Amott cell were transferred to clean containers. Then, the core was taken from the Amott cell and placed inside the core holder. The aqueous solution was injected into the core holder at a constant flow rate at 347 K. The outlet pressure was constant at the atmospheric pressure. The produced oil and water were collected outside the oven. The produced oleic-phase volume and pressure drop along the core were recorded periodically. Once the water cut reached 100%, the injection rate was increased to reduce the capillary end effect. The recovered oil amount by the forced imbibition by 1.1- wt% 3pRB was determined by quantitative ^{1}H NMR that gave the 3p concentration in the recovered oil.

According to Rapoport and Leas, the capillary effect can be neglected when the scaling coefficient $Lu\mu_w$ is greater than 0.5–3.5 cm^2 cp/min, in which L is the length of the core sample, u is the injection rate, and μ_w is the viscosity of the aqueous solution [47,48]. For the forced imbibition with RB, the injection rate was 32 cm^3/h, which gave the Rapoport-Leas scaling coefficient of 0.8 cm^2 cp/min and the capillary number of 9.0×10^{-7}. The oil production became undetectable after 5 pore volumes of injection (PVI). Then, the injection rate was increased to 257 cm^3/h, which gives the Rapoport Leas scaling coefficient of 6.0 cm^2 cp/min and the capillary number of 7.2×10^{-6}.

For the forced imbibition with 3pRB, the injection rate was 32 cm^3/h, which gave the Rapoport-Leas scaling coefficient of 0.7 cm^2 cp/min and the capillary number of 8.3×10^{-7}. The water-cut became 100% after 10 PVI. Then, the increased injection rate of 129 cm^3/h gave the Rapoport Leas scaling coefficient of 2.8 cm^2 cp/min and the capillary number of 3.3×10^{-6}. No additional oil was recovered by the increased injection rate.

3. Results and discussion

This section presents the main results of the contact angle, IFT, density, viscosity, and imbibition experiments. The oil recovery results from the imbibition experiment are explained by several important mechanisms of 3pRB.

3.1. Contact-angle experiments

As described in Section 2.3, two aqueous solutions were tested, RB and 1.1- wt% 3pRB (the 3p solubility limit), at 347 K. Fig. 7 shows the change in contact angle with the two solutions. For the RB case (Fig. 7a), the initial average contact angle was 105°, but an equilibrium state after 24 h gave a contact angle of 123°. That is, RB did not reduce the contact angle.

Fig. 7b shows the results for 1.1- wt% 3pRB. The initial average contact angle was 95°. It rapidly decreased to 74° within 2 h, and then gradually decreased to 26° at 66 h, rendering the calcite surface strongly water-wet. After 3 days, no oil droplets were observed on the calcite surface. Fig. 8 compares the average contact angles for the tested solutions, and shows the rapid reduction in contact angle by 1.1- wt% 3pRB, especially for the initial few hours.

The mechanism of wettability alteration by 3pRB is related to the carbonyl oxygen of 3p that is electron rich because of the inductive electron donation from two alkyl groups. The electron-rich oxygen atom of 3p can reduce the interaction of positively charged rock surfaces and the carboxylate groups that anchor the oil to the surface. This dipole-ion interaction between the 3p molecules and the calcite surface likely caused the wettability to change from oil-wet to strongly water-wet, and the partial or complete detachment of oil molecules from the surface. Note that this interaction between 3p molecules and the calcite surface are expected through the aqueous and oleic phases because 3p partitions into both phases.

3.2. IFT experiments

Section 2.4 described the four fluid systems tested. Table 4 shows the IFT values for the four fluid systems. For system 1, no net mass transfer was expected between the phases during the experiment. For system 2, water could be transferred from 1.1- wt% 3pRB to the 3p-rich phase. The IFT value for system 2 was estimated by using the densities of 3p and 1.1- wt% 3pRB.

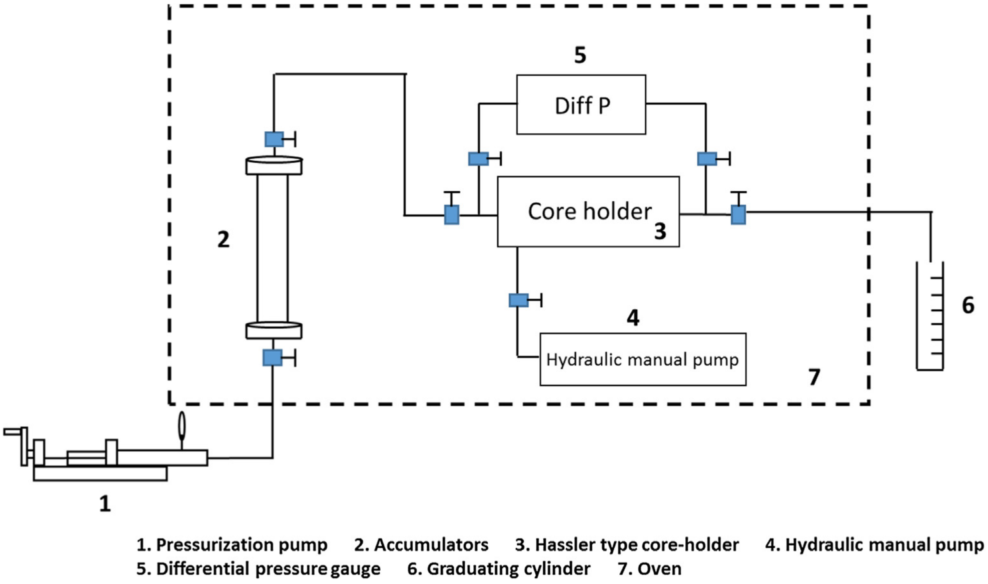

Fig. 6. Schematic of the experimental set up for the forced imbibition (Section 2.7).

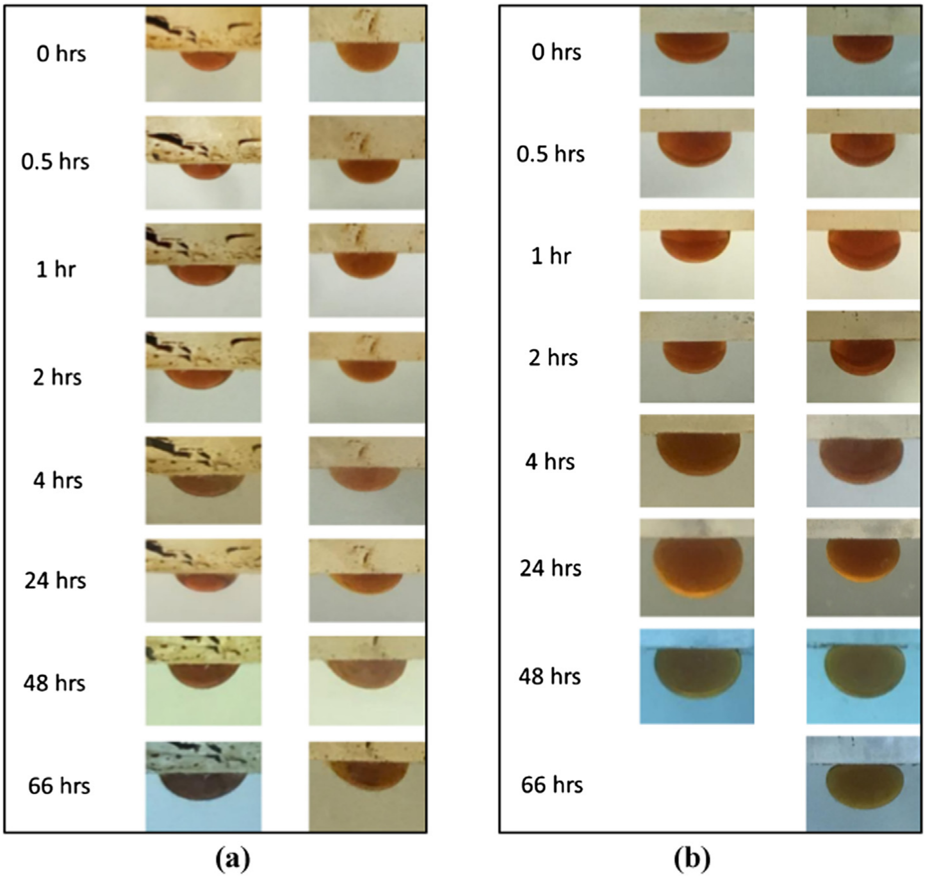

Fig. 7. Change in contact angle for oil droplets in (a) RB and (b) 1.1- wt% 3pRB (the solubility limit at 347 K). They were all at 347 K and atmospheric pressure. One of the oil droplets for 3pRB was detached from the surface after 48 h.

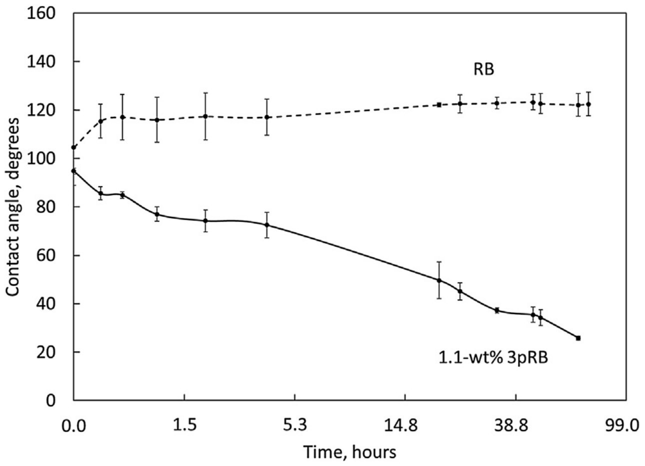

Fig. 8. Contact angles measured for the reservoir brine (RB) (Table 2) and 1.1-wt% 3pRB at 347 K and atmospheric pressure. Standard deviations of contact angles are shown as the error bars in the figure. The contact angle rapidly decreased with 1.1- wt% 3pRB within a few hours of the experiment commencement.

Table 4
IFT for four systems at 347 K and atmospheric pressure: (1) crude oil and RB, (2) 3p and 1.1- wt% 3pRB, (3) crude oil and 1.1- wt% 3pRB, and (4) crude oil diluted by 18.6 wt% 3p and 0.8- wt% 3pRB.

	Sample name and its density at 347 K, kg/m^3		IFT, mN/m
System 1	Crude oil	780	11.44
	Reservoir brine	1030	
System 2	3-Pentanone	760	10.02
	1.1- wt% 3pRB	1030	
System 3	Crude oil with no 3p	780	11.05
	1.1- wt% 3pRB	1030	
	3-Pentanone with no crude oil	760	11.94
	1.1- wt% 3pRB	1030	
System 4	Crude oil diluted with 18.6 wt% 3-pentanone	772	10.68
	0.8- wt% 3pRB	1030	

For system 3, it is likely that the mass transfer of 3p occurred from the aqueous to the oleic phase during the experiment. Therefore, a range of IFTs was estimated by using the upper and lower limit density values for the oleic phase. The upper and lower limits in density for the oleic phase are the crude oil density and 3p density, respectively. For the aqueous phase density, both 1.1- wt% 3pRB and RB were measured to be 1030 kg/m^3. Among the fluid systems given in Table 4, system 3 is most relevant to the proposed method of oil recovery by injection of 1.1- wt% 3pRB.

These results show that the presence of 3p had essentially no effect on the IFT between the oleic and the aqueous phases. The impact of 3p on the IFT was limited because of the small amount of 3p in the aqueous phase at the experimental condition (i.e., 1.1 wt% in this experiment). This result indicates that the reduction in contact angle measured for 3pRB was a consequence of wettability alteration for the nearly constant IFT around 11 mN/m.

3.3. Density and viscosity experiments

Tables 5 and 6 provide the densities and viscosities measured for the three mixtures of crude oil and 3p as described in Section 2.5. They are

Table 5
The densities of crude oil and its mixtures with 3-pentanone.

0 wt% 3-Pentanone (344 K)		18.6 wt% (33 mol%) 3-Pentanone (347 K)		41.0 wt% (60 mol%) 3-Pentanone (347 K)		64.9 wt% (80 mol%) 3-Pentanone (347 K)	
Pressure, kPa	Density, kg/m^3	Pressure, kPa	Density, kg/m^3	Pressure, kPa	Density, kg/m^3	Pressure, kPa	Density, kg/m^3
96.53	782.1819	103.97	771.8049	107.01	768.9360	101.01	765.4374
999.74	782.9128	1385.02	773.0452	1379.02	770.3187	1383.02	766.7794
4998.70	786.3198	3452.00	775.0159	3447.03	772.3546	3445.03	769.0788
9997.40	790.2524	6899.03	778.2247	6891.03	775.7424	6896.00	772.6733
17140.37	795.5964	10345.03	781.3632	10343.03	779.0497	10342.00	776.2332

also shown in Figs. 9 and 10(a). Table 5 and Fig. 9 show that the mixture density slightly decreases with increasing 3p concentration and decreasing pressure.

Table 6 and Fig. 10(a) show that the oleic-phase viscosity decreased with increasing 3p concentration. Comparison of the original oil viscosity with the viscosity of 64.9 wt% (80 mol%) 3p and 35.1 wt% oil indicates a viscosity reduction by a factor between two and three. The oil viscosity reduction can improve the oil recovery rate during the imbibition of 3pRB, as will be further analyzed with scaling theory in the next subsection.

3.4. Spontaneous imbibition

The imbibition experiment with 1.1- wt% 3pRB was compared with that with RB as the base case at 347 K. No oil recovery was observed when the core samples were immersed in the solutions. This indicated that the cores were oil-wet after the aging at 347 K for 3 weeks. The experiment was concluded within two weeks after confirmation of no more oil recovery.

Fig. 11 compares the oil recovery factors obtained by the spontaneous imbibition with RB and 1.1- wt% 3pRB at 347 K. The oil recovery factor from the oil-aged limestone core reached 45% at 2 days and the final oil recovery of 51.0% in the 3pRB case. In contrast, the final oil recovery was 12.0% in the RB case.

As given in Section 2.6, the initial concentration of 3p in RB was 1.1 wt% (the solubility of 3p in RB at the experimental pressure and temperature). After the experiment, the 3p concentration was 18.6 wt% in the recovered oleic phase and 0.8 wt% in the aqueous phase outside the core. This confirmed the mass transfer of 3p from the aqueous phase to the oleic phase, causing oil viscosity reduction and oil swelling by 3p. It is unknown how the 3p amount inside the core was distributed under a transient non-equilibrium state during the experiment.

Fig. 12 shows that oil was produced from the top of the core in the RB case, indicating the contribution of buoyancy to oil recovery. Fig. 13 shows that oil was produced not only from the top, but also from the side surface of the core in the 3pRB case. This indicates that the counter- and co-current flow contributed to the oil recovery with 3pRB likely because of the wettability alteration without affecting the water/oil IFT, oil swelling, and oil viscosity reduction in addition to the buoyant force. Fig. 13 also shows that 3pRB created no emulsion.

Since this imbibition experiment was a capillary dominated process, Ma et al.'s scaling theory

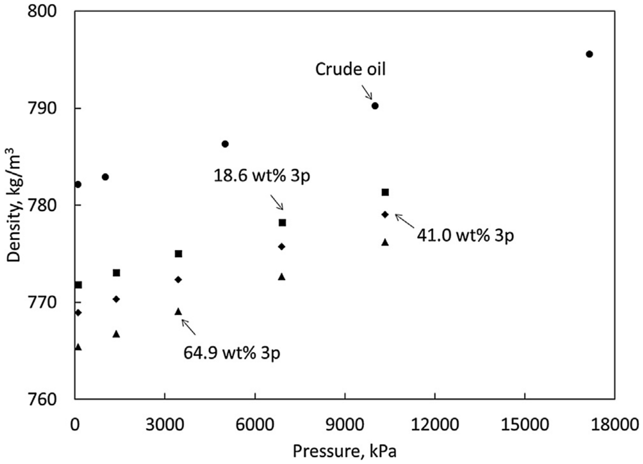

Fig. 9. Densities of crude oil and its mixtures with 3-pentanone. The crude oil densities were measured at 344 K. All other densities were measured at 347 K.

$$t_d = t\sqrt{\frac{k}{\phi}}\frac{\sigma}{\sqrt{\mu_o\mu_w}}\frac{4(d^2+2L^2)}{L^2d^2} \tag{2}$$

was used to estimate the contribution from the viscosity reduction by 3p [49]. In Eq. (2), t_d is dimensionless time, t is time, ϕ is porosity, k is permeability, σ is interfacial tension, μ_w and μ_o are aqueous phase viscosity and oleic phase viscosity, d is core diameter and L is core length. This equation indicates that the oil recovery rate is proportional to ${\mu_o}^{-1/2}$. As shown in Fig. 10(b), ${\mu_o}^{-1/2}$ increases with increasing 3p concentration. ${\mu_o}^{-1/2}$ of the crude oil is 1.0987 cp$^{-1/2}$ at 344 K and atmospheric pressure, and ${\mu_o}^{-1/2}$ of 3p-diluted oil (33 mol% or 18.6 wt %) is 1.2383 cp$^{-1/2}$ at 347 K and atmospheric pressure. These results indicate that the oil recovery rate during this particular imbibition experiment could have been enhanced by 13% because of the oil dilution by 3p. In addition to viscosity reduction, 3p can also cause oil swelling. Oleic phase saturation could have been increased by 24% when the oil was diluted by 18.6 wt% 3p at 347 K and atmospheric pressure.

3.5. Forced imbibition

As described in Section 2.7, the forced imbibition was performed for

Table 6
The viscosity of crude oil and its mixtures with 3-pentanone.

0 wt% 3-Pentanone (344 K)		18.6 wt% (33 mol%) 3-Pentanone (347 K)		41.0 wt% (60 mol%) 3-Pentanone (347 K)		64.9 wt% (80 mol%) 3-Pentanone (347 K)	
Pressure, kPa	Viscosity, cp	Pressure, kPa	Viscosity, cp	Pressure, kPa	Viscosity, cp	Pressure, kPa	Viscosity, cp
96.53	0.8284*	134.38	0.6522	157.89	0.4609	135.90	0.3267
999.74	0.8450	1381.57	0.6534	1375.71	0.4604	1381.57	0.3264
4998.70	0.9090	3448.00	0.6533	3448.00	0.4596	3446.55	0.3242
9997.40	0.9950	6887.59	0.6545	6889.10	0.4613	6893.45	0.3221
17140.37	1.1150	10336.00	0.6561	10337.52	0.4592	10340.41	0.3205

* This value was extrapolated from the crude oil viscosities at 344 K and 999.74 kPa–17140.37 kPa.

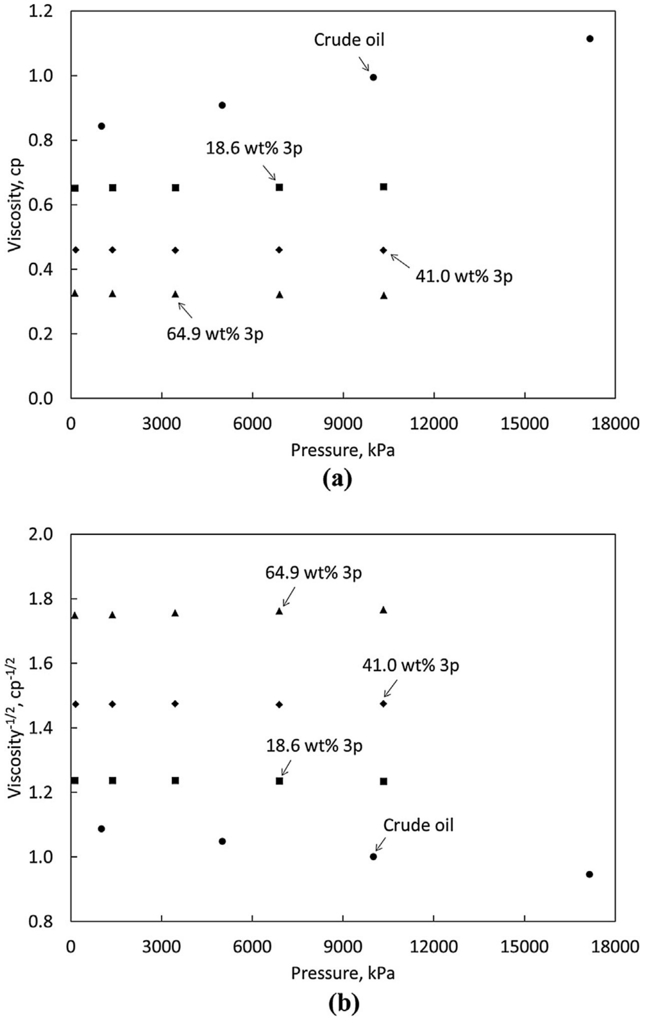

Fig. 10. (a) Viscosities of crude oil and its mixtures with 3-pentanone (3p). The crude oil viscosities were measured at 344 K and the other viscosities were measured at 347 K. (b) Viscosity$^{-1/2}$ of crude oil and its mixtures with 3p. Oil recovery rate by capillary-driven water imbibition is estimated to be proportional to $\mu_o{}^{-1/2}$, which increases with increasing 3p concentration.

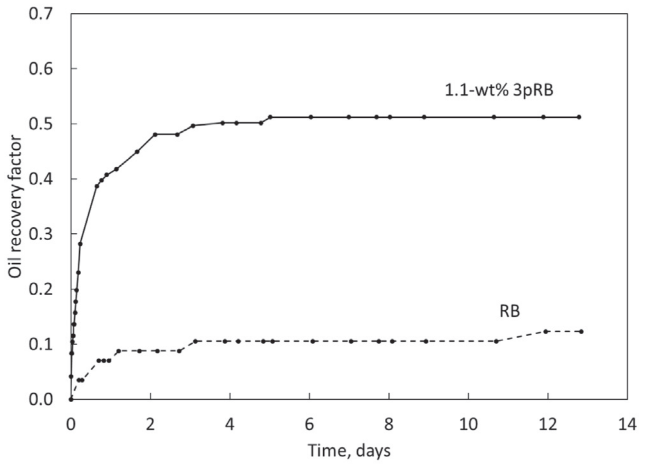

(a) Oil recovery factors with respect to time

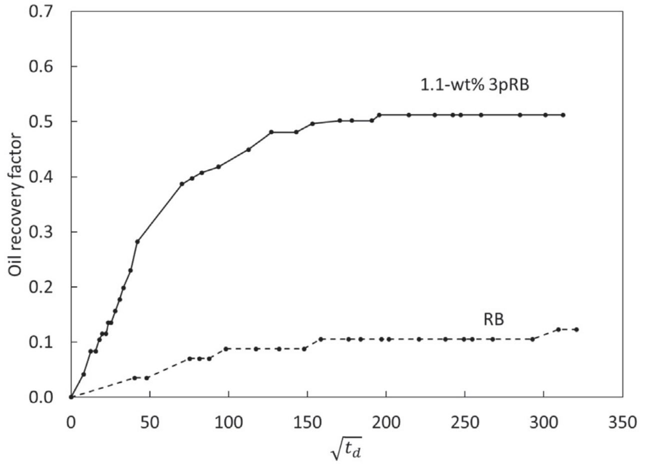

(b) Oil recovery factors with respect to the square root of dimensionless time (t_d)

Fig. 11. Oil recovery factors from the spontaneous imbibition experiments with RB and 1.1- wt% 3pRB at 347 K. The oil recovery factor reached 50.0% with 3pRB and 10.0% with RB at Day 3, and 51.0% with 3pRB and 11.0% in RB at Day 5. These cores were subject to the forced imbibition experiment, as shown in Fig. 14. Dimensionless time (t_d) for 1.1- wt% 3pRB was calculated with crude oil viscosity at 347 K and atmospheric pressure; however, the oleic phase viscosity actually decreases during imbibition as the transfer of 3p takes place from the aqueous to the oleic phase.

the cores after the spontaneous imbibition at 347 K. Fig. 14 shows the oil recovery by the forced imbibition of RB and 1.1- wt% 3pRB. In this figure, the oil recovery factors at “0 PVI” are the final oil factors from the spontaneous imbibition. For the RB case, the oil recovery factor from the forced imbibition leveled off at 36.5% after 4.2 PVI at the flow rate of 32 cm^3/h. An additional oil recovery of 3.3% was obtained by the increased injection rate, which made the total oil recovery factor of 51.8% (12.0% with the spontaneous imbibition and 36.5% + 3.3% with the forced imbibition). The Amott index to water for this core was calculated to be 0.23 based on the oil recovery factor of 39.8% by the forced imbibition.

For the 3pRB case, the produced oil during each time step was less than 0.5 ml after 2 PVI, and tended to stick on the wall of the receiver vial. The forced imbibition was paused after 5 PVI to quantify oil recovery at each time step. Then, the forced imbibition was resumed for the 2nd batch of injection. It was possible that the phase distribution changed between the 1st and 2nd batch of injection. This is likely the reason for the change in the trend in the oil recovery factor around 5 PVI for the 3pRB case in Fig. 14. The oil recovery factor of this forced imbibition was 16.5% at 10 PVI.

The Amott index to water was calculated to be 0.76, which is much greater than the Amott index to water for the RB case, 0.23. This result indicates a clear, positive impact of 3pRB on oil recovery by water imbibition in the cores tested. However, we recognize that this is a consequence of multiple mechanisms caused by the presence of 3p; that is, it is not only because the wettability was changed from oil-wet to strongly water-wet without lowering the oil/RB IFT, but also because the miscibility between 3p and crude oil caused oil swelling and oil viscosity reduction. Furthermore, these two factors might have some synergistic effect because the miscibility of 3p with oil could allow the access of 3p molecules to oil-wet surfaces through the two immiscible liquid phases.

The results in this paper collectively showed a potential of improved oil recovery by the 3p additive to RB in mixed-wet or oil-wet rock formations. Although this paper was focused on 3p, the molecular structure of ketone can be optimized for a given set of reservoir and operating conditions. This multifunctional solvent is environmentally friendly and commercially available. It can be injected as an additive to aqueous or gaseous injection fluids. It can partition into all fluid phases (oleic, gaseous, and aqueous) and also interact with positively charged oil-wet surfaces once it is injected into the formation. More data are to

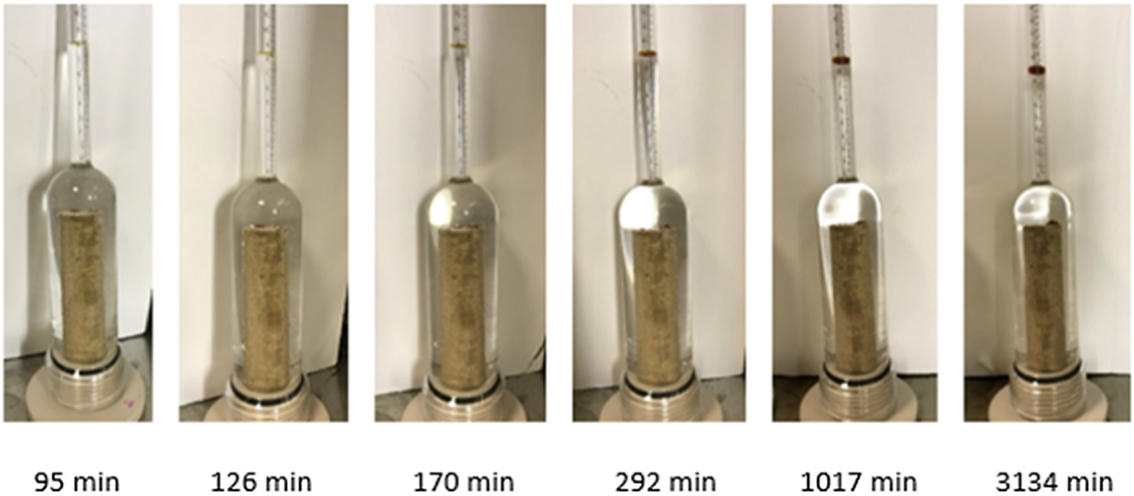

Fig. 12. Spontaneous imbibition experiment with RB at 347 K. It was observed that oil was produced from the top face of the core, indicating the contribution of buoyancy force.

be obtained for fundamental properties of mixtures of 3p with various oil and/or brine samples at a wide range of pressure and temperature conditions. Oil recovery experiments with various cores of different mineralogy types are also to be performed, such as huff-n-puff experiments using aqueous or gaseous injection fluids with ketone as an additive.

4. Conclusions

This paper presented for the first time an investigation of 3-pentanone (3p) as an additive to reservoir brine (RB) for improved oil recovery from mixed- or oil-wet cores. Two sets of imbibition experiments using oil-aged limestone cores were performed with RB and 1.1- wt% 3p in RB (3pRB) at 347 K. This 3pRB was at the solubility limit of 3p in RB at 347 K, which defined the maximum concentration of 3p in this research. Oil recovery results were explained on the basis of more fundamental experiments, such as contact-angle, IFT, viscosity, and density experiments. Conclusions are as follows:

1. The contact angle experiment showed that 3pRB can rapidly alter the wettability of oil-aged calcite surfaces from an oil-wet to a strongly-water-wet state at 347 K. The final contact angle observed was 26° with 3pRB, in contrast to 123° with RB. The IFT experiment indicated that the presence of 3p did not affect the IFT between crude oil and RB during the contact angle experiment. That is, the wettability change by 3pRB occurred without affecting the IFT between the aqueous and oleic phases.
2. Results from the spontaneous imbibition experiment showed that the oil recovery factor reached 50.0% with 3pRB and 10.0% with RB at Day 3. The final oil recovery factor in the spontaneous imbibition was 51.0% with 3pRB and 12.0% with RB. The spontaneous imbibition rapidly exhibited the clear advantage of 3pRB over RB within the first few days.
3. The subsequent forced imbibition yielded the final oil recovery factor of 67.5% (51.0% with the spontaneous imbibition + 16.5% with the forced imbibition) with 3pRB, and 51.8% (12.0% with the spontaneous imbibition and 36.5% + 3.3% with the forced imbibition) with RB. These results gave the Amott index to water of 0.76 with 3pRB, in contrast to 0.23 with RB. This indicates a clear, positive impact of 3pRB on oil recovery by water imbibition in the cores tested. The main mechanism at play is the wettability change as demonstrated by the contact-angle experiment. Additional

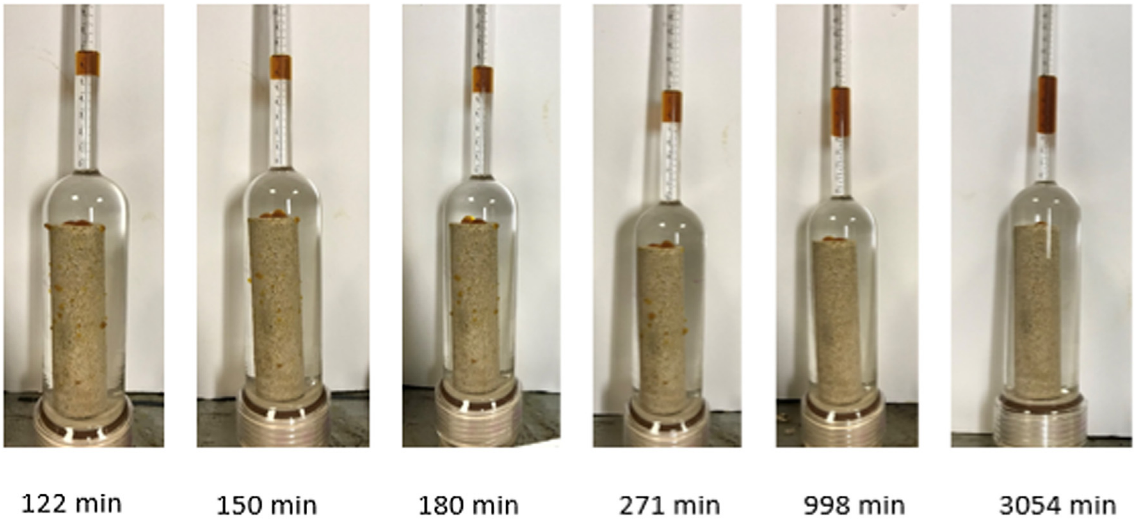

Fig. 13. Spontaneous imbibition experiment with 1.1- wt% 3pRB at 347 K. It was observed that oil was produced not only from the top, but also from the side surface of the core. This indicates that the counter- and co-current flow contributed to the oil recovery with 3pRB, because of the wettability alteration without affecting the water/oil IFT, oil swelling, and oil viscosity reduction in addition to the buoyancy force.

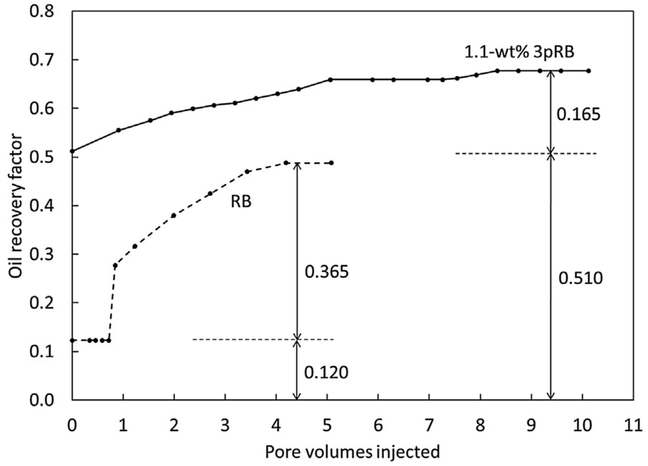

Fig. 14. Oil recovery factor during the forced imbibition with RB and 1.1- wt% 3pRB at 347 K. The oil recovery factors indicated for "0 PVI" are the final oil recovery factors from spontaneous imbibition. For the RB case, the oil recovery factor from forced imbibition leveled off at 36.5% after 4.2 PVI. An additional oil recovery of 3.3% was obtained by the increased injection rate after 5 PVI. The Amott index to water for the RB case was calculated to be 0.23 based on the spontaneous and forced imbibition experiments. For 3pRB case, the produced oil during each time segment was less than 0.5 ml after 2 PVI, and tended to stick on the wall of the receiver vial. Therefore, the experiment was paused after 5 PVI to quantify the oil recovery at each time step. After the measurement of the produced oil mass from 0 to 5 PVI, the experiment was resumed for the 2nd batch of injection. It is likely that the phase distribution in the core was altered while preparing the 2nd batch injection of 3pRB. The Amott index to water for the 3pRB case was calculated to be 0.76 based on the spontaneous and forced imbibition experiments.

mechanisms include the miscibility of 3p with oil that yielded oil swelling and oil viscosity reduction.

4. It is conceivable that the wettability change caused by 3pRB is related to the dipole-ion interaction between the 3p molecules and the calcite surface. This interaction may reduce the polar-polar interaction of the carboxylate group of naphthenic acids in oil with the calcite surface. The partitioning of 3p into the oleic and aqueous phases may increase the accessibility of 3p to rock surfaces through the two liquid phases and, therefore, increase the possibility for 3p's electron-rich oxygen atom to interact with positively-charged rock surfaces.
5. When 3p is dissolved in the oil, it enhances the oil mobility through the oil swelling and viscosity reduction as is the case with conventional miscible solvents. The oil viscosity was reduced by 21% when the oil was diluted by 18.6 wt% (33 mol%) 3-pentanone at 347 K. Calculation results showed that this oil viscosity reduction could improve the oil recovery rate by 13% during the spontaneous imbibition experiment.
6. In the RB tested in this research, the dissolution of 3p did not cause any salt precipitation within the 3p solubility limit (1.1 wt%) at 347 K. This makes 3p desirable as an additive to a RB-based aqueous injection fluid. It is possible to select an optimal ketone solvent for a given set of reservoir and operating conditions in terms of the oil recovery mechanisms discussed in this paper.

Acknowledgement

Ryosuke Okuno holds the Pioneer Corporation Faculty Fellowship in Petroleum Engineering at The University of Texas at Austin.

References

[1] Yan R, Lieskovsky J, Gorgen S. New eagle ford wells continue to show higher production. U.S. Energy Information Administration; 2014 [accessed 15 April 2019]. https://www.eia.gov/todayinenergy/detail.php?id=18171.

[2] Hoffman BT. Huff-N-puff gas injection pilot projects in the eagle ford. .Presented at SPE Canada unconventional resources conference, Calgary, Alberta, Canada, 13–14 March SPE-189816-MS; 2018. https://doi.org/10.2118/189816-MS.

[3] Clark AJ. Determination of recovery factor in the bakken formation, Mountrail County, ND. Presented at SPE annual technical conference and exhibition, New Orleans, Louisiana, USA, 4-7 October SPE-133719-STU; 2009. https://doi.org/10.2118/133719-STU.

[4] Alharthy N, Teklu T, Kazemi H, Graves R, Hawthorne S, Braunberger J, et al. Enhanced oil recovery in liquid-rich shale reservoirs: laboratory to field. Presented at SPE annual technical conference and exhibition, Houston, Texas, USA SPE-175034-MS; 2015. p. 28–30. https://doi.org/10.2118/175034-MS.

[5] Barba RE. Liquids rich organic shale recovery factor application. Presented at SPE annual technical conference and exhibition, Houston, Texas, USA, 28-30 September SPE-174994-MS; 2015. https://doi.org/10.2118/174994-MS.

[6] Hoffman BT, Evans JG. Improved oil recovery IOR pilot projects in the bakken formation. Presented at SPE low perm symposium, Denver, Colorado, USA, 5-6 May SPE-180270-MS; 2016. https://doi.org/10.2118/180270-MS.

[7] Alfarge D, Wei M, Bai B. IOR methods in unconventional reservoirs of North America: comprehensive review. Presented at SPE western regional meeting, Bakersfield, California, USA, 23-27 April SPE-185640-MS; 2017. https://doi.org/10.2118/185640-MS.

[8] Ground Water Protection Council and ALL Consulting. Modern shale gas development in the United States: a primer. Washington, DC: U.S. Department of Energy; 2009.

[9] Nelson PH. Pore-throat sizes in sandstones, tight sandstones, and shales. AAPG Bull 2009;93(03):329–40.

[10] Mullen J. Petrophysical characterization of the eagle ford shale in South Texas. Presented at Canadian unconventional resources and international petroleum conference, Calgary, Alberta, Canada, 19-21 October SPE-138145-MS; 2010. https://doi.org/10.2118/138145-MS.

[11] Alvarez JO, Tovar FD, Schechter DS. Improving oil recovery in the wolfcamp reservoir by soaking/flowback production schedule with surfactant additives. SPE Reservoir Eval Eng 2018;21(04):1083–96. https://doi.org/10.2118/187483-PA. SPE-187483-PA.

[12] Alvarez JO, Saputra IWR, Schechter DS. The impact of surfactant imbibition and adsorption for improving oil recovery in the wolfcamp and eagle ford reservoirs. SPE J 2018;23(06):2103–17. https://doi.org/10.2118/187176-PA. SPE-187176-PA.

[13] Buckley JS, Liu Y, Monsterleet S. Mechanisms of wetting alteration by crude oils. SPE J 1998;3(01):54–61. https://doi.org/10.2118/37230-PA. SPE-37230-PA.

[14] Alvarez JO, Schechter DS. Wettability, oil and rock characterization of the most important unconventional liquid reservoirs in the United States and the impact on oil recovery. Presented at unconventional resources technology conference, San Antonio, Texas, USA, 1-3 August URTEC-2461651-MS; 2016. https://doi.org/10.15530/URTEC-2016-2461651.

[15] Morsy S, Sheng JJ, Soliman MY. Waterflooding in the eagle ford shale formation: experimental and simulation study. Presented at SPE Unconventional Resources Conference and Exhibition-Asia Pacific, Brisbane, Australia, 11–13 November SPE-167056-MS; 2013. https://doi.org/10.2118/167056-MS.

[16] Alvarez JO, Schechter DS. Wettability alteration and spontaneous imbibition in unconventional liquid reservoirs by surfactant additives. SPE Reservoir Eval Eng 2017;20(01):107–17. https://doi.org/10.2118/177057-PA. SPE-177057-PA.

[17] Lu Y, Najafabadi NF, Firoozabadi A. Effect of low-concentration of 1-pentanol on the wettability of petroleum fluid-brine-rock systems. Langmuir 2019;35(12):4263–9.

[18] Shuler PJ, Tang H, Lu Z, Tang Y. Chemical process for improved oil recovery from Bakken Shale. Presented at Canadian unconventional resources conference, Calgary, Alberta, Canada, 15-17 November SPE-147531-MS; 2011. https://doi.org/10.2118/147531-MS.

[19] Wang D, Butler R, Zhang J, Seright R. Wettability survey in Bakken Shale with surfactant-formulation imbibition. SPE Reservoir Eval Eng 2012;15(06):695–705. https://doi.org/10.2118/153853-PA. SPE-153853-PA.

[20] Kathel P, Mohanty KK. Wettability alteration in a tight oil reservoir. Energy Fuels 2013;27(11):6460–8.

[21] Alvarez JO, Neog A, Jais A, Schechter DS. Impact of surfactants for wettability alteration in stimulation fluids and the potential for surfactant EOR in unconventional liquid reservoirs. Presented at SPE unconventional resources conference, The Woodlands, Texas, USA, 1-3 April SPE-169001-MS; 2014. https://doi.org/10.2118/169001-MS.

[22] Nguyen D, Wang D, Oladapo A, Zhang J, Sickorez J, Butler R, Mueller B. Evaluation of surfactants for oil recovery potential in shale reservoirs. Presented at SPE improved oil recovery symposium, Tulsa, Oklahoma, USA, 12-16 April SPE-169085-MS; 2014. https://doi.org/10.2118/169085-MS.

[23] Zeng T, Miller CS, Mohanty KK. Application of surfactants in shale chemical EOR at high temperatures. Presented at the SPE improved oil recovery conference, Tulsa, Oklahoma, USA, 14-18 April SPE-190318-MS; 2018. https://doi.org/10.2118/190318-MS.

[24] Liang T, Longoria RA, Lu J, Nguyen QP, DiCarlo DA. Enhancing hydrocarbon permeability after hydraulic fracturing: laboratory evaluations of shut-ins and surfactant additives. SPE J 2017;22(04):1011–23. https://doi.org/10.2118/175101-PA. SPE-175101-PA.

[25] Adibhatla B, Mohanty KK. Parametric analysis of surfactant-aided imbibition in fractured carbonates. J Colloid Interface Sci 2008;317(02):513–22.

[26] Gupta R, Mohanty KK. Temperature effects on surfactant-aided imbibition into fractured carbonates. SPE J 2010;15(03):588–97. https://doi.org/10.2118/

110204-PA. SPE-110204-PA.

[27] Tu J, Sheng JJ. Experimental and numerical study of shale oil EOR by surfactant additives in fracturing fluid. Presented at the unconventional resources technology conference, Denver, Colorado, USA, 22-24 July URTeC-2019-295; 2019. https://doi.org/10.105530/urtec-2019-295.

[28] Lu J, Britton C, Solairaj S, Liyanage PJ, Kim DH, Adkins S, et al. Novel large-hydrophobe alkoxy carboxylate surfactants for enhanced oil recovery. SPE J 2014;19(06):1024–34. https://doi.org/10.2118/154261-PA. SPE-154261-PA.

[29] Mirzaei M, Dicarlo D. Imbibition of anionic surfactant solution into oil-wet capillary tubes. Transp Porous Media 2013;99(01):37–54.

[30] Baek K, Argüelles-Vivas FJ, Abeykoon GA, Okuno R, Weerasooriya UP. Application of novel surfactants with co-solvent character for heavy oil recovery. Presented at the SPE western regional meeting, San Jose, California, USA, 23-26 April SPE-195345-MS; 2019. https://doi.org/10.2118/195345-MS.

[31] Liu J, Sheng JJ, Wang X, Ge H, Yao E. Experimental study of wettability alteration and spontaneous imbibition in Chinese shale oil reservoirs using anionic and nonionic surfactants. J Petrol Sci Eng 2019;175:624–33.

[32] Liu J, Sheng JJ, Huang W. Experimental investigation of microscopic mechanisms of surfactant-enhanced spontaneous imbibition in shale cores. Energy Fuel 2019;33(8):7188–99.

[33] Valluri MK, Alvarez JO, Schechter DS. Study of the rock/fluid interactions of sodium and calcium brines with ultra-tight rock surfaces and their impact on improving oil recovery by spontaneous imbibition. Presented at the SPE Low Perm Symposium, Denver, Colorado, USA, 5-6 May SPE-180274-MS; 2016. https://doi.org/10.2118/180274-MS.

[34] Austad T, Strand S, Madland MV, Puntervold T, Korsnes RI. Seawater in chalk: an EOR and compaction fluid. SPE Reservoir Eval Eng 2008;11(04):648–54. https://doi.org/10.2118/118431-PA. SPE-118431-PA.

[35] Olsen AL, Washburn ER. A study of solutions of isopropyl alcohol in benzene, in water and in benzene and water. J Am Chem Soc 1935;57(2):303–5.

[36] Farouq Ali SM, Stahl CD. Computer models for simulating alcohol displacement in porous media. SPE-1037-PA SPE J 1965;5(01):89–99. https://doi.org/10.2118/1037-PA.

[37] Al-Wahaibi YM, Grattoni CA, Muggeridge AH. Physical properties (density, viscosity, surface tension, interfacial tension, and contact angle) of the system isopropyl alcohol + cyclohexane + water. J Chem Eng Data 2007;52:548–52. https://doi.org/10.1021/je060442b.

[38] Collerson RR, Counsell JF, Handley R, Martin JF, Sprake CHS. Thermodynamic properties of organic oxygen compounds. Part XV. Purification and vapour pressures of some ketones and ethers. J Chem Soc (Resumed) 1965:3697–700.

[39] Daubert TE, Danner RP. Data compilation tables of properties of pure compounds. New York: American Institute of Chemical Engineers; 1985.

[40] Stephenson RM. Mutual solubilities: water-ketones, water-ethers, and water-gasoline-alcohols. J Chem Eng Data 1992;37(1):80–95.

[41] Vasou V. Density of oil-related systems at high pressures [Master thesis] Lyngby, Denmark: Technical University of Denmark; 2015.

[42] Cambridge Viscosity and Petroleum Analyzer Company (PAC). ViscoPro 2100 viscometer operational manual revision C. Houston, Texas: PAC; 2018.

[43] Schechter DS, Zhou D, Orr Jr. FM. Low IFT drainage and imbibition. J Petrol Sci Eng 1994;11(4):283–300.

[44] Zhou D, Stenby EH. Immiscible displacement in a porous medium simulated by a statistical model. In: Buller AT, Berg E, Hjelmeland O, Kleppe J, Torsæter O, Aasen JO, editors. North sea oil and gas reservoirs – II. Dordrecht: Springer; 1989. p. 271–80.

[45] Ghosh P, Mohanty KK. Study of surfactant-polymer flooding in high-temperature and high-salinity carbonate rocks. Energy Fuels 2019;33:4130–45.

[46] Churcher PL, French PR, Shaw JC. Rock properties of berea sandstone, baker dolomite, and indiana limestone. Presented at the SPE international symposium on oilfield chemistry, Anaheim, California, 20-22 February SPE-21044-MS; 1991. https://doi.org/10.2118/21044-MS.

[47] Rapoport LA, Leas WJ. Properties of linear waterfloods. J Petrol Technol 1953;5(05):139–48. https://doi.org/10.2118/213-G. SPE-213-G.

[48] Lake LW, Johns RT, Rossen WR, Pope GA. Fundamentals of enhanced oil recovery. Richardson, Texas: Society of Petroleum Engineers; 2014.

[49] Ma S, Morrow NR, Zhang X. Generalized scaling of spontaneous imbibition data for strongly water-wet systems. Presented at the petroleum conference of the South Saskatchewan section, Regina, Saskatchewan, Canada, 16-18 October PETSOC-95-138; 1995. https://doi.org/10.2118/95-138.